

PACS 61.43.Fs, 61.46.Bc, 77.84.Bw, 78.30.Ly

Raman spectroscopy and X-ray diffraction studies of $(\text{GeS}_2)_{100-x}(\text{SbSI})_x$ glasses and composites on their basis

V.M. Rubish¹, V.O. Stefanovich², V.M. Maryan¹, O.A. Mykaylo², P.P. Shtets¹, D.I. Kaynts², I.M. Yurkin²

¹*Uzhgorod Scientific-Technological Center of the Institute for Information Recording, NAS of Ukraine, 4a, Zamkovi skhody str., 88000 Uzhgorod, Ukraine, e-mail: center.uzh@gmail.com*

²*Uzhgorod National University, 3, Narodna sq., Uzhgorod 88000, Ukraine*

Abstract. The structure and structural changes under the isothermal annealing of $(\text{GeS}_2)_{100-x}(\text{SbSI})_x$ ($0 \leq x \leq 90$) glasses were investigated by Raman spectroscopy and X-ray diffraction methods. The nanoheterogeneous nature of these glasses structure has been revealed. The matrix of $(\text{GeS}_2)_{100-x}(\text{SbSI})_x$ glasses is basically built just of binary GeS_4 , SbS_3 and SbI_3 structural groups and contains a small amount of molecular fragments with homopolar Ge–Ge and S–S bonds. The phase structure arising in the glass matrix at crystallization corresponds to the structure of crystalline SbSI.

Keywords: chalcogenide glasses, Raman spectra, local structure, ferroelectric, nanocomposites.

Manuscript received 20.11.13; revised version received 30.01.14; accepted for publication 20.03.14; published online 31.03.14.

1. Introduction

Obtaining and studying $(\text{GeS}_2)_{100-x}(\text{SbSI})_x$ glasses and their amorphous films are important in view of both fundamental and practical aspects. Due to their high sensitivity, GeS_2 non-crystalline materials are potential candidates for being used as optical information storage media, gratings, optical diffraction elements, holographic recording media, etc. [1-5]. Ferroelectric-semiconductor antimony sulphoiodide (SbSI) shows excellent properties [6] and is a promising material for various applications (infrared, piezo- and pyroelectric detectors, actuators, memory, etc. [7 – 9]).

$(\text{GeS}_2)_{100-x}(\text{SbSI})_x$ ($0 \leq x \leq 90$) glasses have been studied with the aim of examining the possibility to obtain some new structures of higher quality in respect of dielectric and optical properties on the basis of materials with amorphous internal network. In view of the fact that the structure and physical properties of non-crystalline materials can be modified in different ways,

first of all, by continuous variation of starting components ratio, and then, by modification of the synthesis regime and subsequent thermal, electric and optical treatment, the main aim was to find out the optimal conditions for obtaining composites with desired properties.

It has been shown that in the matrix of GeS_2 -SbSI glasses under certain thermal treatment SbSI crystalline inclusions could be obtained [10-12]. There is also a report on fabrication of antimony sulphoiodide crystalline inclusions in the matrix of $(\text{GeS}_2)_{100-x}(\text{SbSI})_x$ glasses under laser beam treatment [13]. In the course of Raman measurements, formation of SbSI crystallites in the As_2S_3 glass matrix was observed [14, 15].

The influence of obtaining SbSI nanocrystalline inclusions and heat treatment conditions on the structure of As_2S_3 -SbSI glasses was earlier revealed [16-18]. It was shown that, in the matrix of glasses obtained under rigid hardening conditions, SbSI nanocrystalline inclusions were absent [16, 17]. In the course of cooling

the melts from lower homogenization temperatures, and, accordingly, at lower cooling rates, the presence of SbSI nanocrystals in the glassy matrix was detected [18]. Similar situation probably occurs also in the GeS_2 -SbSI system [19]. The features within the range $115 - 138 \text{ cm}^{-1}$, identified in Raman spectra of annealed glasses containing 50–90 mol% of SbSI, indicate the presence of the nanocrystalline inclusions of antimony sulphoiodide in these materials.

In this paper, we report the studies of the structure of $(\text{GeS}_2)_{100-x}(\text{SbSI})_x$ ($0 \leq x \leq 90$) glasses obtained under rigid hardening conditions and the structural changes that occur in them under the annealing process.

2. Experimental

$(\text{GeS}_2)_{100-x}(\text{SbSI})_x$ ($0 \leq x \leq 90$) glasses were prepared by using the vacuum melting method ($\sim 0.01 \text{ Pa}$) of the relevant mixture of GeS_2 and SbSI components, preliminarily synthesized from the high-purity elemental substances. The weight of samples was chosen depending on the composition of alloys within 3–10 g. Glassy GeS_2 was obtained by cooling the homogenized melt (for 72 h) from 1100 K in cold water. Polycrystalline SbSI was prepared by cooling the homogenized melt (for 72 h) from 900 K in the turned-off furnace regime. $(\text{GeS}_2)_{100-x}(\text{SbSI})_x$ melts were homogenized at 900–1100 K for 48 h. The melts were periodically stirred. Cooling of these melts also was carried out in cold water. The obtained glasses were not annealed. Amorphous nature of the glasses were verified using the X-ray diffraction analysis (Fig. 1).

The Raman spectra were obtained at $T = 293 \text{ K}$ with 1 cm^{-1} resolution by using a DFS-24 spectrophotometer and He-Ne laser ($\lambda = 632.8 \text{ nm}$). The power of laser radiation was set as low as possible to avoid photostructural transformations in the samples at their heating.

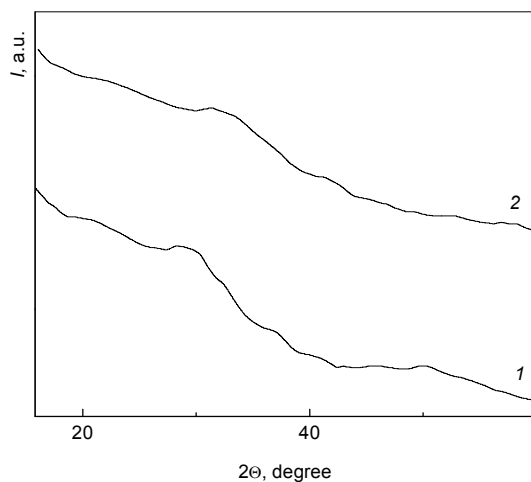


Fig. 1. X-ray powder diffraction patterns of as-prepared $(\text{GeS}_2)_{50}(\text{SbSI})_{50}$ (1) and $(\text{GeS}_2)_{30}(\text{SbSI})_{70}$ (2) glasses.

X-ray diffraction studies of glasses, crystallized glasses and polycrystalline SbSI were carried out using DRON-3 X-ray apparatus. CuK_α -radiation ($\lambda = 1.5418 \text{ \AA}$) was applied.

3. Results and discussion

In the Raman spectra of $(\text{GeS}_2)_{100-x}(\text{SbSI})_x$ glasses, the broad features typical for amorphous materials are observed. As it is seen from the curve 1 in Fig. 2, the Raman spectrum of GeS_2 unannealed glass contains rather intense broad bands at $101, 343, 373$ and 441 cm^{-1} as well as less pronounced features at $200, 255$ and 500 cm^{-1} . Earlier, we studied the Raman spectrum of GeS_2 glass annealed at $T_g - 20 \text{ K}$ (T_g – glass transition temperature) [20]. In this case, the feature at 255 cm^{-1} in the Raman spectrum for this glass was not detected, and the feature at 500 cm^{-1} is less pronounced. The obtained results are in good agreement with the results of other authors [21–23].

The intense bands at $343, 373$ and 441 cm^{-1} correspond to atom vibrations in $\text{Ge}(\text{S}_{1/2})_4$ tetrahedra that form an extensive 3D spatial structural network of GeS_2 glass. According to [24–26], the basis of the GeS_2 glass matrix is the chains of $\text{Ge}(\text{S}_{1/2})_4$ tetrahedra that are bound by vertices and joined (also in vertices) by the bridge tetrahedra. The link between tetrahedra is realized through two coordinated S atoms. Deformation vibrations of $\text{Ge}(\text{S}_{1/2})_4$ tetrahedra may cause the band in the range of 200 cm^{-1} . Within the same range of frequencies, the vibrations of S_n fragments [20, 24, 25] are active. The broad band at 100 cm^{-1} may be associated with the deformation vibrations in fragments of chains of glassy GeS_2 .

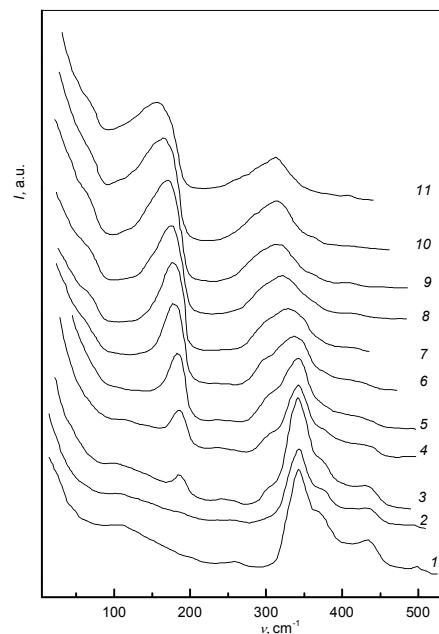


Fig. 2. Raman spectra of as-prepared $(\text{GeS}_2)_{100-x}(\text{SbSI})_x$ glasses. x , mol.%: 0 (1), 5 (2), 10 (3), 20 (4), 30 (5), 40 (6), 50 (7), 60 (8), 70 (9), 80 (10), 90 (11).

The weak band at 500 cm^{-1} (Fig. 2, curve 1) shows the presence of either short chains of sulfur or S–S interconnected bridges between tetrahedra in the GeS_2 glass network. The presence of S–S homopolar bonds in the glass matrix suggests the existence of Ge–Ge bonds in it. Accordingly, the weak band in the Raman spectrum at 255 cm^{-1} may indicate the presence of the ethane-like $\text{Ge}(\text{S}_{1/2})_6$ nanophase in the glassy GeS_2 matrix [20, 23]. It is confirmed by the results of Raman spectra of glassy Ge_2S_3 [20] and $\text{Ge}_x\text{S}_{100-x}$ glasses when $x > 33.3$ [20, 22]. With increase of the Ge content in $\text{Ge}_x\text{S}_{100-x}$ glasses, the intensity of the bands at 255 cm^{-1} goes up significantly [22]. In addition, at 230 cm^{-1} in the Raman spectra of these glasses, there observed is the feature that relates to the nanophase of distorted salt $\text{Ge}(\text{S}_{1/6})_6$ [23]. In the Raman spectrum of glassy Ge_2S_3 , the intensity of these bands is significant. This behavior of Raman spectra of $\text{Ge}_x\text{S}_{100-x}$ glasses can be explained by the assumption that with increasing concentration of Ge tetrahedra, they behave like “going into” each other. It follows that germanium sulfides up to $x \leq 40$ consist mainly of structural units $\text{GeS}_{4/2}$ and $\text{Ge}_2\text{S}_{6/2}$ ($\text{S}_3\text{Ge-GeS}_3$), connected to the spatial network through divalent sulfur atoms or through short chains of S_n .

Incorporation of SbSI in GeS_2 leads to essential changes in Raman spectra. In the Raman spectrum of $(\text{GeS}_2)_{95}(\text{SbSI})_5$ glass, in addition to the bands characteristic for GeS_2 glass (Fig. 2, curve 1), the weak band at 188 cm^{-1} and the features at 238 and 300 cm^{-1} (Fig. 2, curve 2) were revealed. The feature at 300 cm^{-1} can be attributed to the vibrations of Sb–S bonds in SbS_3 pyramids. Meanwhile, the similar bond near 300 cm^{-1} , related to the vibrations of $\text{SbS}_{3/2}$ structural units, was observed in Raman spectra of Sb_2S_3 thin films [27], glasses of Sb–S and Sb_2S_3 - SbSI_3 systems [20, 28, 29] and in the infrared absorption spectra of glassy SbSI [30]. The bands at 238 and 254 cm^{-1} (present in the spectrum of GeS_2 glass) according to [20] are referred to homopolar Ge–Ge bonds. The appearance of the band at 300 cm^{-1} indicates that in the structural network, built mainly by $\text{GeS}_{4/2}$ tetrahedra, $\text{SbS}_{3/2}$ structural groups are formed. The bond between them is realized through the sulfur atoms.

The band at 188 cm^{-1} indicates to the presence of structural SbI_3 groups in the glass matrix. Significant increase of this band intensity and its shift in the short-wave region of the spectrum with increasing SbSI content in glasses of the GeS_2 -SbSI system (Fig. 2, curves 2–11) proves in favor of this assumption. The maximum of this band for $(\text{GeS}_2)_{10}(\text{SbSI})_{90}$ glass is localized at 163 cm^{-1} (Fig. 2, curve 11). The similar Raman features related to the vibrations of SbI_3 structural units were reported for the glasses of Sb_2S_3 - SbI_3 [29], Sb_2S_3 -AsSI [30] and As_2S_3 -SbSI [14-17] systems. Also, the sharp band at 157 cm^{-1} in the Raman spectrum of polycrystalline SbI_3 is observed [16]. The Raman spectra of $(\text{GeS}_2)_{100-x}(\text{SbSI})_x$ glasses do not show any evidence for the presence of GeI_4 molecular groups in their matrix. According to [31], the intense band at 148 cm^{-1} in the Raman spectra of $\text{Ge}_x\text{S}_y\text{I}_z$ glasses

corresponds to the vibrations of Ge and I atoms in GeI_4 structural groups.

With the increase of antimony sulphoiodide concentration in the composition of $(\text{GeS}_2)_{100-x}(\text{SbSI})_x$ glasses, the intensity of high-frequency bands ($\nu > 340\text{ cm}^{-1}$) appropriately decreases and the intensity of bands at 300 cm^{-1} grows. Simultaneously, they shift in the low-frequency spectrum range. The bands at 230 – 260 cm^{-1} almost disappear. It indicates the absence of the structural units of $\text{GeS}_{3-x}\text{I}_x$ – $\text{SbSI}_{3/2}$ and $\text{GeS}_{4-x}\text{I}_x$ ($1 \leq x \leq 4$) in the matrix of $(\text{GeS}_2)_{100-x}(\text{SbSI})_x$ glasses. The possibility of formation of these units in the glasses of this system was indicated in [19].

With the growth of SbSI content in the composition of glasses, there is a gradual transition from the structure based on $\text{GeS}_{4/2}$ tetrahedral units to the structure based on $\text{SbS}_{3/2}$ pyramids. The bond between structural groups is specified through the sulfur atoms. The increase of the number of mixed ($\text{GeS}_{4/2}$ - $\text{SbS}_{3/2}$) structural units in the matrix of glasses of the GeS_2 -SbSI system leads to the shift of the main band in the Raman spectra into the low frequency region. For example, for $(\text{GeS}_2)_{10}(\text{SbSI})_{90}$ glass, the maximum of the high-frequency band is observed at 315 cm^{-1} (Fig. 2, curve 11). At the same time, there is an association process of structural SbI_3 groups. Smearing of main bands in Raman spectra of glasses with a high content of antimony sulphoiodide confirms a significant structural disorder in the glasses network. The features that could indicate the existence of the chain ternary structural $\text{SbS}_{2/2}\text{I}$ units building crystalline SbSI [6, 32] in the glassy matrix were not observed in Raman spectra of $(\text{GeS}_2)_{100-x}(\text{SbSI})_x$ glasses.

As a result of Raman spectroscopy studies, it was concluded that the $(\text{GeS}_2)_{100-x}(\text{SbSI})_x$ glasses have the nanoheterogeneous structure. The matrix of these glasses is basically built just of binary GeS_4 , SbS_3 and SbI_3 structural groups and also contains small amounts of molecular fragments with homopolar Ge–Ge and S–S bonds.

The obtained data are different from the results of the structure studies for $(\text{GeS}_2)_{100-x}(\text{SbSI})_x$ ($50 \leq x \leq 90$) glasses given in [19]. In Raman spectra of the glasses presented in this work, there are intense bands at 115 , 138 , 165 and 315 cm^{-1} and a less pronounced band at 290 cm^{-1} (for glasses with $x = 50, 60, 70$). The similar bands (107 – 110 and 138 – 140 cm^{-1}) are observed in the Raman spectra of the bulk crystal [33, 34] and polycrystalline SbSI (Fig. 3, curve 1), also in the crystallized glasses of As_2S_3 -SbSI, As_2Se_3 -SbSI and Sb_2S_3 -AsSI systems [16-18, 30, 35]. This fact may testify the presence of nanocrystalline SbSI inclusions in the matrix of $(\text{GeS}_2)_{100-x}(\text{SbSI})_x$ glasses which were obtained by the authors [19].

The difference between the Raman spectra results presented in [19] and those presented in this work is due to the differences in sample preparation techniques for the measurement. In [19], the glasses of the GeS_2 -SbSI

system, obtained by cooling the melts in cold water from $T = 793$ K and annealed for 2 h at $T = 413$ K, were studied. In our studies, unannealed glasses derived by cooling the melts in cold water from the homogenization temperatures (900–1100 K) were used. In the course of cooling the melts from lower temperatures, and, accordingly, at lower cooling rates, it was not possible to completely suppress the processes of nucleation and crystal growth. Furthermore, it can point out that SbSI crystal inclusions could be formed in the glass matrix at the annealing process of glasses.

Earlier [36], $(\text{GeS}_2)_{100-x}(\text{SbSI})_x$ glasses were investigated by differential thermal analysis (DTA). DTA curves were taken at the heating rate of 6 K/min. On DTA curves for glasses with $x > 50$, two exothermic effects were detected, and the intensity of the first one was much smaller than of the other. For example, for $(\text{GeS}_2)_{20}(\text{SbSI})_{80}$ glass, the temperatures maxima of these effects are 400 and 509 K, respectively. In addition, it was found that the maximum temperature of the first effect of crystallization of $(\text{GeS}_2)_{100-x}(\text{SbSI})_x$ glasses ($50 \leq x \leq 90$) weakly depends on the composition, and it is within 395–405 K. At these temperatures, crystalline inclusions of antimony sulphoiodide are formed in the glasses. The investigation results of $(\text{GeS}_2)_{10}(\text{SbSI})_{90}$ glass, annealed at 413 K for 1 h, using Raman spectroscopy and X-ray diffraction, confirm this conclusion [12, 36].

Here, we present the data studies of the annealing effect on the structure of $(\text{GeS}_2)_{100-x}(\text{SbSI})_x$ glasses with the content of antimony sulphoiodide 50 and 70 mol.%. On X-ray powder diffraction patterns there are reflexes (Fig. 3, curves 2, 3) for the glasses of referred compositions after annealing at 403 K for 2 h, indicating the presence of crystalline phases. In the same figure, a fragment of the diffraction pattern of polycrystalline SbSI (Fig. 3, curve 1) is given.

It is seen that they have weak reflexes, positions of which satisfactorily coincide with the positions of intense lines in the diffraction pattern of polycrystalline SbSI. This is the evidence that the phase structure arising in the $(\text{GeS}_2)_{100-x}(\text{SbSI})_x$ glass matrix during their crystallization conforms the structure of crystalline antimony sulphoiodide.

The same conclusion follows from the results of the Raman spectra research of these glasses. Presented in Fig. 4 (curves 2, 3) are the Raman spectra of $(\text{GeS}_2)_{50}(\text{SbSI})_{50}$ and $(\text{GeS}_2)_{30}(\text{SbSI})_{70}$ glasses crystallized at 403 K for 2 h. In the same figure, the Raman spectrum of polycrystalline SbSI (Fig. 4, curve 1) is given. Raman spectra of crystallized glasses have sharp bands at 109–110, 139–140 and 319–320 cm^{-1} and weak features at 166–169, 208–210, 255–257 cm^{-1} . The similar bands are observed in the Raman spectra of mono- [33, 34], poly- (Fig. 4, curve 1) and nano- [37, 38] crystalline SbSI.

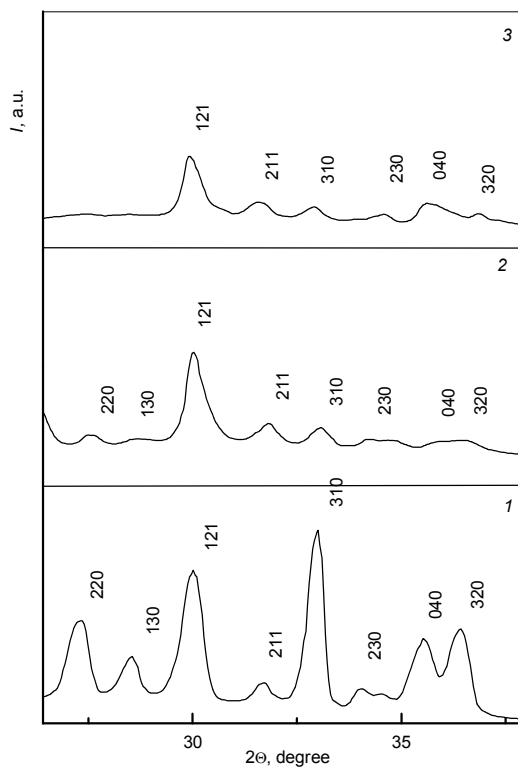


Fig. 3. Fragments of X-ray powder diffraction patterns of polycrystalline SbSI (1) and annealed at $T = 403$ K for 2 h $(\text{GeS}_2)_{30}(\text{SbSI})_{70}$ (2) and $(\text{GeS}_2)_{50}(\text{SbSI})_{50}$ (3) glasses.

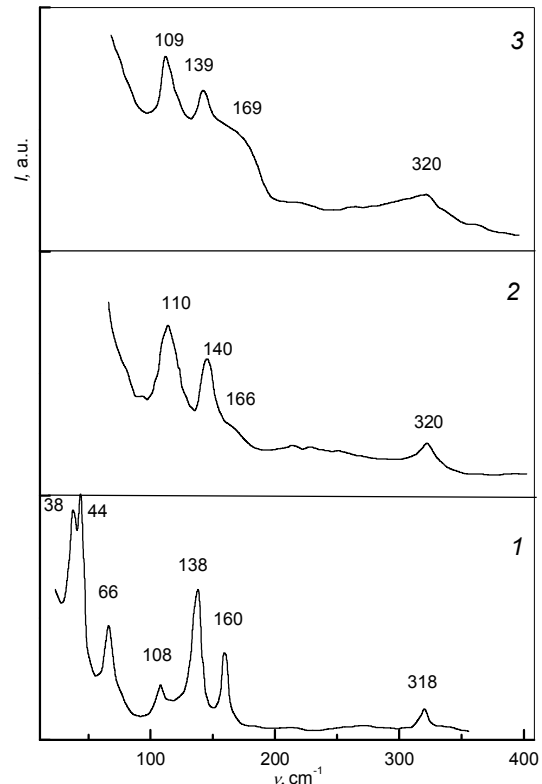


Fig. 4. Raman spectra of polycrystalline SbSI (1) and annealed at $T = 403$ K for 2 h $(\text{GeS}_2)_{30}(\text{SbSI})_{70}$ (2) and $(\text{GeS}_2)_{50}(\text{SbSI})_{50}$ (3) glasses.

It was shown above that the glasses of the GeS₂-SbSI system have the nanoheterogeneous structure. Their matrix is built only by binary structural units GeS_{4/2} and SbS_{3/2} and contains SbI₃ molecules or is associated on their basis. Also, there are structural fragments with homopolar bonds Ge-Ge and S-S in the matrix of glasses. During the heating process of (GeS₂)_{100-x}(SbSI)_x glasses up to the temperatures of the 1-st exothermic effect, maximum breaking and switching of Ge-Ge, S-S, Ge-S, Sb-S, Sb-I chemical bonds are possible in these binary structural groups. This process is accompanied by diffusion of atoms. As a result, the chain ternary SbS_{2/2}I groups, which are characteristic for SbSI crystals, are formed in the glassy matrix.

4. Conclusion

(GeS₂)_{100-x}(SbSI)_x (0 ≤ x ≤ 90) glasses have been obtained under rigid hardening conditions. It was established that the glasses of these systems have the nanoheterogeneous structure. Their matrix is built only by binary structural units GeS_{4/2} and SbS_{3/2} and contains molecular SbI₃ fragments and a small amount of structural groups with homopolar bonds. The restructuring process in glasses, held in them during annealing, leads to the structural relaxation, accompanied by breaking and switching of chemical bonds in these binary structural groups and formation of SbSI crystalline inclusions.

References

1. R.R. Gerke, T.G. Dubrovina, M.D. Mikhailov, Obtaining holographic diffraction gratings on light-sensitive layers of chalcogenide glasses by dry etching // *J. Opt. Technol.* **64**(11), p. 1008-1012 (1997).
2. K. Petkov, Compositional dependence of the photoinduced phenomena in thin chalcogenide films // *J. Optoelectron. Adv. Mat.* **4**(3), p. 611-629 (2002).
3. R. Todorov, Tz. Iliev, K. Petkov, Light-induced changes in the optical properties of thin films of Ge-S-Bi (Te, In) chalcogenides // *J. Non-Cryst. Solids.* **326&327**, p. 263-267 (2003).
4. K. Naohiko, F. Tatsuo, T. Akihiro et al., GeS₂/metal thin film bilayered structures as write-once-type optical recording materials // *J. Appl. Phys.* **100**(11), 113115 (2006).
5. V.M. Maryan, G.T. Horvat, M.M. Pop et al., Photostimulated changes in the optical properties of sulphides germanium and arsenic thin films // *Phys. Chem. Solid State*, **9**(3), p. 524-528 (2008), in Ukrainian.
6. V.M. Fridkin, *Ferroelectrics Semiconductors*. Consultants Bureau, New York, 1980.
7. P. Mural, Micromachined infrared detectors based on pyroelectric thin films // *Repts. Progr. Phys.* **64**(10), p. 1339-1388 (2001).
8. S. Surthi, S. Kotru, R.K. Pandey, SbSI films for ferroelectric memory applications // *Integr. Ferroelectr.* **48** (1), p. 263-269 (2002).
9. M. Nowak, P. Mroczek, P. Duka et al., Using of textured polycrystalline SbSI in actuators // *Sens. Actuators A Phys.* **150**(2), p. 251-256 (2009).
10. V.M. Rubish, Anomalous behaviour of dielectric permittivity of chalcogenide glasses in crystallization temperature range // *Sensors Electronics and Microsystems Technologies*, **1**, p. 62-66 (2007), in Ukrainian.
11. V.M. Rubish, Obtaining and crystallization peculiarities of glasses on the antimony sulfoiodide basis // *Phys. Chem. Solid State*, **8**(1), p. 41-46 (2007), in Ukrainian.
12. V.M. Rubish, M.Yu. Rigan, S.M. Gasinets et al., Obtaining and crystallization peculiarities of antimony sulphoiodide containing chalcogenide glasses // *Ferroelectrics*, **372**(1), p. 87-92 (2008).
13. P. Gupta, A. Stone, N. Woodward et al., Laser fabrication of semiconducting ferroelectric single crystal SbSI features on chalcogenide glass // *Opt. Mater. Exp.* **1**(4), p. 652-657 (2011).
14. Yu.M. Azhniuk, P. Bhandivad, V.M. Rubish et al., Photoinduced changes in the structure of As₂S₃-based SbSI nanocrystal-containing composites studied by Raman spectroscopy // *Ferroelectrics*, **416**, p. 113-118 (2011).
15. Yu.M. Azhniuk, V. Stoyka, I. Petryshynets et al., SbSI nanocrystal formation in As-Sb-S-I glass under laser beam // *Mater. Res. Bull.* **47**, p. 1520-1522 (2012).
16. V.M. Rubish, V.O. Stefanovich, O.G. Guranich et al., Structure investigation of As-Sb-S-I system glasses by Raman spectroscopy // *Nanosystems, Nanomaterials, Nanotechnologies*, **6**(4), p. 1119-1127 (2008), in Ukrainian.
17. M. Barj, O.A. Mykaylo, D.I. Kaynts et al., Formation and structure of crystalline inclusions in As₂S₃-SbSI and As₂Se₃-SbSI systems glass matrices // *J. Non-Cryst. Solids*, **357**, p. 2232-2234 (2011).
18. V.M. Rubish, L. Bih, O.A. Mykaylo et al., The influence of obtaining and heat treatment conditions on the structure of As₂S₃-SbSI system // *Semiconductor Physics, Quantum Electronics & Optoelectronics*, **16**(2), p. 123-127 (2013).
19. L. Ding, D. Zhad, H. Jain et al., Structure of GeS₂-SbSI glasses by Raman spectroscopy // *J. Amer. Ceram. Soc.* **93**(10), p. 2932-2934 (2010).
20. V.V. Petrov, A.A. Kryuchin, V.M. Rubish, *Materials for Perspective Optoelectronic Devices*. Naukova dumka-Verlag, Kiev, 2012 (in Russian).
21. P. Boolchand, J. Grathaus, M. Tenhaver et al., Structure of GeS₂ glass: Spectroscopic evidence for broken chemical order // *Phys. Rev. B*, **33**(8), p. 5421-5434 (1986).

22. I.P. Kotsalas, C. Raptis. Structural Raman studies of $\text{Ge}_x\text{S}_{1-x}$ chalcogenide glasses // *J. Optoelectron. Adv. Mat.* **3**(3), p. 675-684 (2001).
23. L. Cai, P. Boolchand, Nanoscale phase separation of GeS_2 glass // *Phil. Mag. B*, **82**(15), p. 1649-1657 (2002).
24. D.I. Bletska, V.S. Gerasimenko, Vibrational spectra and the structure of glasses of Ge-Bi-S system // *Phys. Chem. Glass.* **13** (3), p. 359-363 (1987), in Russian.
25. P.P. Shtets, V.I. Fedelech, V.M. Kabatsij et al., Structure, dielectric and photoelastic properties of glasses in the system Ge-Sb-S // *J. Optoelectron. Adv. Mat.* **3**(4), p. 937-940 (2001).
26. A. Feltz, *Amorphous and Vitreous Inorganic Solids*. Mir, Moscow, 1986 (in Russian).
27. B. Frumarova, M. Bilkova, M. Frumar et al., Thin films of Sb_2S_3 doped by Sm^{3+} ions // *J. Non-Cryst. Solids*, **326-327**, p. 348-352 (2003).
28. V.M. Rubish, A.P. Shpak, V.I. Malesh, Investigation of the short-range order structure of antimony-sulfur system glasses by the methods of vibration and X-ray diffraction spectroscopy // *Nanosystems, Nanomaterials, Nanotechnologies*, **5**(1), p. 189-202 (2007), in Ukrainian.
29. I.D. Turjanitsa, L.K. Vodop'yanov, V.M. Rubish et al., Raman spectra and dielectric properties of glasses of Sb-S-I system // *J. Appl. Spectrosc.* **44**(5), p. 501-504 (1985), in Russian.
30. V.M. Rubish, V.M. Marjan, V.O. Stefanovich et al., Formation mechanism and nature of crystalline inclusions in the matrix of Sb_2S_3 -AsSI system glasses // *Phys. Chem. Solid State*, **14**(1), p. 70-74 (2003), in Ukrainian.
31. L. Koudelka, M. Pisarcik, Raman study of short range order in $\text{Ge}_x\text{S}_y\text{I}_z$ glasses // *J. Non-Cryst. Solids*, **113**, p. 239-245 (1989).
32. J. Grigas, E. Talik, V. Lasauskas, Splitting of the XPS in ferroelectric SbSI crystals // *Ferroelectrics*, **284**, p. 147-160 (2003).
33. C.H. Perry, D.K. Agrawal, The Raman spectrum of ferroelectric SbSI // *Solid State Commun.* **8**, p. 225-230 (1970).
34. M.K. Teng, M. Balcanski, M. Massot et al., Optical phonon analysis in the $\text{A}_v\text{B}_{VI}\text{C}_{VII}$ compounds // *Phys. Stat. Solidi (b)*, **62**, p. 173-182 (1974).
35. D.I. Kaynts, A.P. Shpak, V.M. Rubish et al., Formation of ferroelectrics nanostructures in $(\text{As}_2\text{S}_3)_{100-x}(\text{SbSI})_x$ glassy matrix // *Ferroelectrics*, **371**(1), p. 28-33 (2008).
36. V.M. Rubish, M.Yu. Rigan, V.P. Perevuznyk et al., Glassforming, crystallization and physico-chemical properties of alloys in systems on the basis of SbSI // *Phys. Chem. Solid State*, **10**(4), p. 861-866 (2009), in Ukrainian.
37. A.V. Gomonnai, I.M. Voynarovych, A.M. Solomon et al., X-ray diffraction and Raman scattering in SbSI nanocrystals // *Mat. Res. Bull.* **38**(13), p. 1767-1772 (2003).
38. I.M. Voynarovych, A.V. Gomonnai, A.M. Solomon et al., Characterization of SbSI nanocrystals by electron microscopy, X-ray diffraction and Raman scattering // *J. Optoelectron. Adv. Mat.* **5**(3), p. 713-718 (2003).